

Quantum criticality of a \mathbb{Z}_3 symmetric spin chain with long-range interactions

Xue-Jia Yu,¹ Chengxiang Ding,² and Limei Xu^{1,3,4,*}

¹*International Center for Quantum Materials, School of Physics, Peking University, Beijing 100871, China*

²*School of Science and Engineering of Mathematics and Physics,
Anhui University of Technology, Maanshan, Anhui 243002, China*

³*Collaborative Innovation Center of Quantum Matter, Beijing, China*

⁴*Interdisciplinary Institute of Light-Element Quantum Materials and Research
Center for Light-Element Advanced Materials, Peking University, Beijing, China*

(Dated: January 23, 2023)

Based on large-scale density matrix renormalization group techniques, we investigate the critical behaviors of quantum three-state Potts chains with long-range interactions. Using fidelity susceptibility as an indicator, we obtain a complete phase diagram of the system. The results show that as the long-range interaction power α increases, the critical points f_c^* shift towards lower values. In addition, the critical threshold $\alpha_c (\approx 1.43)$ of the long-range interaction power is obtained for the first time by a non-perturbative numerical method. This indicates that the critical behavior of the system can be naturally divided into two distinct universality classes, namely the long-range ($\alpha < \alpha_c$) and short-range ($\alpha > \alpha_c$) universality classes, qualitatively consistent with the classical ϕ^3 effective field theory. This work provides a useful reference for further research on phase transitions in quantum spin chains with long-range interaction.

I. INTRODUCTION

Quantum phase transitions (QPTs) are phase transitions between quantum matters at zero temperature by tuning athermal parameters, which can be a first-order phase transition represented by some sudden abrupt jump behavior or a continuous phase transition described by a critical exponent. Universality class categorized by critical points or unstable fixed points in the sense of renormalization group (RG) [1] is a core concept in QPTs. Using field theory or numerical exact approaches, conventional or unconventional QPT can be described by constructing simplified effective lattice models [2–4]. Therefore, quantum many-body systems with nearest-neighbor interactions, such as the transverse field Ising model, Heisenberg model, and Hubbard model, are of fundamental importance for understanding QPTs and universality classes [5]. A well-known QPT is the second-order Ising transition in the one-dimensional transverse field Ising model, and its critical exponents are perfectly supported by experimental results [5].

Quantum systems with long-range interactions, such as Coulomb interaction ($1/r_{ij}$) [6], dipole-dipole interaction ($1/r_{ij}^3$) [7, 8], and van der Waals interaction ($1/r_{ij}^6$) [6], have attracted widespread attention in recent years, accompanied by significant advances in experimental techniques for manipulating quantum simulators, such as atomic, molecular and optical systems [8–12]. For instance, tunable power-law interactions $1/r^{d+\alpha}$ with a power $0 \leq \alpha + d \leq 3$ are realized in trapped ions [13–17], which provides a perfect platform for studying novel physics of quantum many-body systems with long-range power-law interaction and stimulated many subsequent many-body physics studies. One example is the neutral Rydberg atom trapped in optical tweezers with programmable van der Waals interactions. It provides promising tunable platforms to explore various novel physics, such as gapped \mathbb{Z}_2 quantum

spin liquids [18–23], quantum phase transitions between different density wave ordered (e.g. \mathbb{Z}_3 ordered) and disordered phases [24–30]. Specifically, the \mathbb{Z}_n symmetric quantum spin model system [31, 32], namely the "parafermion" model system, favors topological phases with more efficient non-Abelian anyon bound states [31, 32], providing a possible approach for universal topological quantum computing, thereby attracting extensive attention and stimulated extensive studies [32–38]. However, despite extensive interest in \mathbb{Z}_n symmetric quantum many-body systems with long-range interactions, it remains challenging to fully understand their critical behavior both theoretically and numerically.

It is well known that a d dimensional quantum system with short-range interactions has a well-known equivalent classical counterpart in $d+1$ dimensions. However, the quantum system with long-range interactions does not have a direct counterpart due to the subtle relationship between classical and quantum critical behaviors. For classical $O(N)$ or \mathbb{Z}_n symmetric spin model systems with long-range interactions [39–48], previous RG calculations show that according to the interaction power α , the critical behavior falls into three universality classes namely, 1) the mean-field universality class when $\alpha \leq d/2$, 2) the long-range universality class when $d/2 < \alpha \leq \alpha_c$, and 3) the short-range universality class for $\alpha > \alpha_c$. Note that region 2) is a 'non-classical' region where the critical behavior is characterized by a peculiar long-range critical exponent $\alpha_c (= 2 - \eta_{SR})$, which can be predicted by perturbative RG calculations with a short-range anomalous exponent η_{SR} [39, 43]. The quantum three-state Potts chain is the simplest example of "parafermion" systems, which shows a continuous phase transition from 'topological phase' (Potts ordered) to trivial phase (disordered), thereby is of crucial important for quantum computing [31, 32, 49, 50]. The question is what is the critical behavior of such quantum Potts chains with long-range interaction in the "non-classical" region, and how to estimate the critical exponent α_c if there is a long-range to short-range universality class crossover.

Fidelity susceptibility is a purely geometric quantity of

* limei.xu@pku.edu.cn

quantum states from quantum information world with an obvious advantage that no prior knowledge of order parameters and symmetry-breaking is required. It has been applied to detect a wide range of QPTs [51–62] induced by a sudden change in the structure of the wave-function. The fidelity susceptibility, defined as the response of the wavefunction overlap of two neighboring ground states with respect to an external field, diverges at the critical point and is almost zero away from the critical point, thus characterizing the QPTs well. For example, experiments detect the QPTs in terms of fidelity susceptibility by using the neutron scattering or angle-resolved photoemission spectroscopy (ARPES) techniques [63]. Here, we investigate the finite-size scaling behavior of the fidelity susceptibility [64–67] in the quantum Potts chain with long-range interactions using the finite-size density-matrix renormalization-group (DMRG) method [68–70] based on the matrix product states (MPS) [70, 71]. The critical long-range interaction power α_c is determined in a non-perturbative way for the first time, providing important insight into phase transitions of quantum spin chains with long-range interaction.

The rest of this paper is organized as follows: in Sec. II contains the lattice model of quantum Potts chain with long-range power-law interaction, the numerical method employed, and the scaling relations of fidelity susceptibility. Sec. III shows the phase diagram of the quantum Potts chain with long-range interaction and the finite-size scaling of the critical behavior, followed by a brief discussion in comparison with previous two-loop RG results. The conclusion is presented in Sec. IV. Additional data for our numerical calculations are provided in the Appendixes.

II. MODEL AND METHODS

A. Quantum Potts chain with long-range interaction

The system of our study is a quantum three-state Potts chain with long-range power-law interactions (see Fig. 1(a)), described by the following Hamiltonian [72, 73]

$$\begin{aligned} H_{LRP} &= H_0 + fH_1 \\ &= -\frac{J}{N(\alpha)} \sum_{i,j} \frac{(\sigma_i^\dagger \sigma_j + \sigma_i \sigma_j^\dagger)}{|i-j|^{d+\alpha}} - f \sum_i (\tau_i + \tau_i^\dagger), \end{aligned} \quad (1)$$

where H_1 and H_0 are the driving and undriving Hamiltonian, respectively. J is the interaction strength, and f represents the external transverse field, parameter α tunes the power of long-range interactions ($\frac{1}{|i-j|^{d+\alpha}}$), and d is the spatial dimension (equal to 1 in our case). $N(\alpha) (= \frac{1}{N-1} \sum_{i,j,i \neq j} \frac{1}{r_{ij}^\alpha})$ is the Kac factor to preserve the Hamiltonian extensive. σ dictates the direction of the watch hand, and τ rotates the watch hand clockwise through a discrete angle $2\pi/3$, as shown in Fig. 1(a). σ and τ satisfy $\sigma_i^3 = I, \tau_i^3 = I$, and $\sigma_i \tau_j = \omega \delta_{ij} \tau_j \sigma_i$, where $\omega = e^{2\pi i/3}$. A global \mathbb{Z}_3 transformation represented by $G = \prod_i \tau_i$ makes the Hamiltonian invariant. The operators are

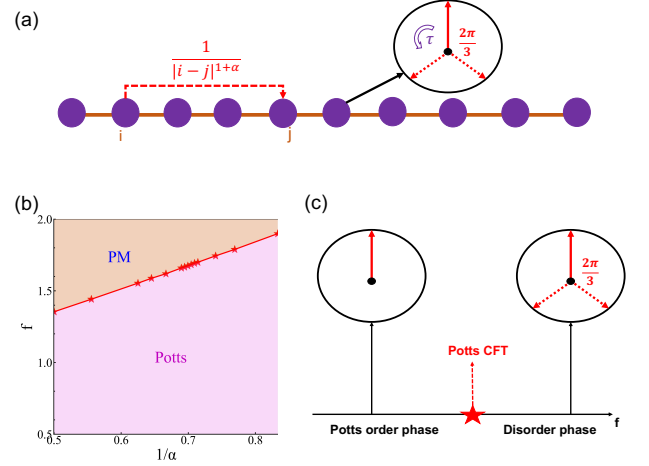


FIG. 1. (Color online) Schematic long-range interaction (a) and ground-state phase diagram with respect to $1/\alpha$ and external transverse field f of quantum Potts chain with long-range interaction (b). In (b), Potts denotes the Potts order phase. PM denotes the paramagnetic disorder phase (see the main text). The red line is the phase boundary between Potts and PM phase, and red star symbols denote the DMRG results of the critical values f_c^* . (c) The schematic phase diagram of standard quantum Potts chain with the nearest-neighbor interaction. The critical point between Potts ordered phase and disordered phase belongs to Potts universality class, which is described by Potts CFT.

defined by

$$\tau = \begin{pmatrix} 1 & 0 & 0 \\ 0 & \omega & 0 \\ 0 & 0 & \omega^2 \end{pmatrix}, \quad \sigma = \begin{pmatrix} 0 & 1 & 0 \\ 0 & 0 & 1 \\ 1 & 0 & 0 \end{pmatrix}. \quad (2)$$

The system is in an ordered phase which breaks the \mathbb{Z}_3 symmetry for $f \ll J$ and in a disordered paramagnetic phase (PM) for $f \gg J$. The phase transition from the \mathbb{Z}_3 -breaking Potts order to the \mathbb{Z}_3 symmetric disordered phase is described by the three-state Potts CFT with correlation length exponent $\nu = 5/6$. The model becomes an infinite-range Potts chain (Lipkin–Meshkov–Glick model [74]) when $\alpha + d = 0$, and a nearest neighbor quantum Potts chain when $\alpha + d = \infty$.

Non-perturbative numerical methods are employed to investigate critical behaviors of quantum Potts chains with long-range power-law interaction and estimate the value of α_c in the "non-classical" region. Inspired by previous RG results for classical systems with long-range interaction [43], only parameter region $1.2 \leq \alpha \leq 2.0$ is considered. Considering that the quantum Potts chain with long-range interaction do not have exact solutions in the parameter region of interest, a large-scale finite-size DMRG method [68–70] based on MPS [70, 71], which is one of the most powerful numerical method for one-dimensional strongly correlated many-body systems, is employed. The MPS bond dimension is set to 300; good convergence of true energy eigenstates and fidelity susceptibilities are guaranteed by requiring relative energy errors less than 10^{-8} . The fidelity susceptibility defined in Eq. 3 is

computed with a minimal step $\delta f = 10^{-3}$. The strength of the interaction $J = 1$ as an energy unit, and open boundary conditions are applied.

B. Fidelity susceptibility and scaling relations

The system undergoes a continuous phase transition from an ordered to a disordered phase when tuning the external field f to a critical value f_c^* , at which the structure of the ground state wave function change significantly. The quantum ground-state fidelity $F(f, f + \delta f)$, defined as the overlapping amplitude of the ground state wave function with the external field f and the ground state wave function with the external field $f + \delta f$ [63–67, 75], and its value is almost zero near f_c^* , that is, $F(f_c^*, f_c^* + \delta f) \sim 0$. In practice, the more convenient quantity to characterize QPTs is the fidelity susceptibility, defined by the leading term of the fidelity,

$$\chi_F(f) = \lim_{\delta f \rightarrow 0} \frac{2(1 - F(f, f + \delta f))}{(\delta f)^2}. \quad (3)$$

For a continuous quantum phase transition of a finite system with size L , fidelity susceptibility exhibits a peak at pseudo-critical point $f_c(L)$, and the value of the quantum critical point f_c^* can be estimated by polynomial fitting $f_c(L) = f_c^* + aL^{-b}$ [76]. In the vicinity of f_c^* , previous studies [51–56, 60, 63, 64] have shown that the finite-size scaling behaviors of fidelity susceptibility $\chi_F(f)$ follows

$$\chi_F(f \rightarrow f_c^*) \propto L^\mu \quad (4)$$

and

$$L^{-d} \chi_F(f) = L^{(2\nu)-d} f_{\chi_F}(L^{1/\nu} |f - f_c^*|), \quad (5)$$

where $\mu (= 2 + 2z - 2\Delta_V)$ is the critical adiabatic dimension [64], z is dynamic exponent, Δ_V is the scaling dimension of the local interaction $V(x)$ at f_c^* , ν is the critical exponent of the correlation length, d is the spatial dimension of the system, and f_{χ_F} is an unknown scaling function. Based on Eq. 4 and 5, the values of critical exponents ν and μ of the QPT can be determined, and the universality class to which the QPT belongs can also be determined. Note that in practice, the critical exponent μ is usually extracted from fidelity susceptibility per site, $\chi_L(f) = \chi_F(f)/L^d$.

III. PHASE DIAGRAM AND CRITICAL BEHAVIOR

A. Quantum phase diagram

The ground state phase diagram of the quantum Potts chain with long-range interactions for $\alpha > 0$ (Eq. 1) is obtained by performing large-scale DMRG simulations with $L = 96, 120, 144, 156, 168, 192, 216, 240$ sites. The result is presented in Fig. 1(b). For $\alpha \rightarrow \infty$, the ground state is a Potts order phase with three-fold degeneracy for $f = 0$ and a paramagnetic disorder phase for $f \rightarrow \infty$, consistent with previous

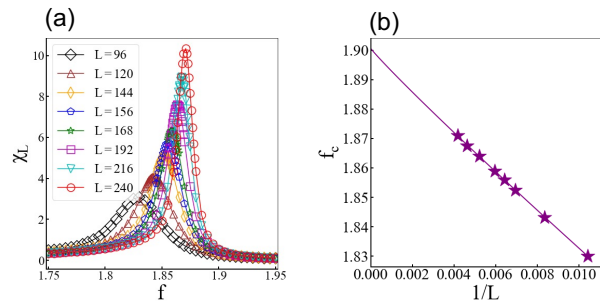


FIG. 2. (Color online) (a) Fidelity susceptibility per site χ_L of the Potts chain with long-range interaction for $\alpha = 1.2$ and $L = 96, 120, 144, 156, 168, 192, 216, 240$ sites as a function of external transverse field f ; symbols denote finite-size DMRG results. (b) Extrapolation of critical point f_c^* for the Potts chain with long-range interaction; symbols denote the finite-size DMRG results for $\alpha = 1.2$ and $L = 96, 120, 144, 156, 168, 192, 216, 240$ sites. We use polynomial fitting $f_c(L) = f_c^* + aL^{-b}$ and extrapolate the critical point $f_c^* = 1.89878$.

results [36](also see Fig. 1(c)). Furthermore, for finite α , it is found that the quantum Potts chain with long-range interactions has a stable Potts order and a disordered phase over the entire range of α we investigate.

The finite-size scaling behavior of fidelity susceptibility for $\alpha = 1.2$ with different L is presented in Figure 2(a), which obeys $\chi_L(f_c^*) \propto L^{\mu-1}$ (Eq. 4) near the second-order QPT critical point. As system size L increases, the peak position $f_c(L)$ gets closer and closer to the exact critical point value f_c^* . More precisely, for the long-range interaction Potts chain with $\alpha = 1.2$, f_c^* is determined by polynomial fitting $f_c(L) = f_c^* + aL^{-b}$, and then extrapolating to L to infinity (Fig. 2(b)). According to Eq. 5, the fidelity susceptibility follows an exact scaling relation, and collapses to one master curve (Fig. 3(b)), confirming that the extrapolation is appropriate. The finite-size scaling behavior of fidelity susceptibility for other α is also investigated (see Appendix A), and the results are presented in Table I. Results show that the quantum critical point moves to lower f_c^* values as α increases.

B. Finite-size scaling and critical exponent

The next questions are what is the critical behavior of the long-range interaction Potts chains with different α values, and whether there is a critical threshold α_c , at which the critical behavior changes continuously from a long-range universality class to a short-range one? To this end, we calculate the critical exponents μ and ν of the fidelity susceptibility in the region $1.2 \leq \alpha \leq 2.0$ based on large-scale DMRG simulations for different L . The value of the fidelity susceptibility per site, $\chi_L = \chi_F/L$, at the peak position $f_c(L) = 1.89878$ for different L at $\alpha = 1.2$ is shown in Fig. 3(a). It can be well fitted by a polynomial fitting of $\chi_L \sim L^\mu(a + bL^{-1})$. According to Eq. 4, the adiabatic critical dimension $\mu = 2.53501$ is then obtained by extrapolation L to infinity.

According to Eq. 5, the fidelity susceptibility can be scaled

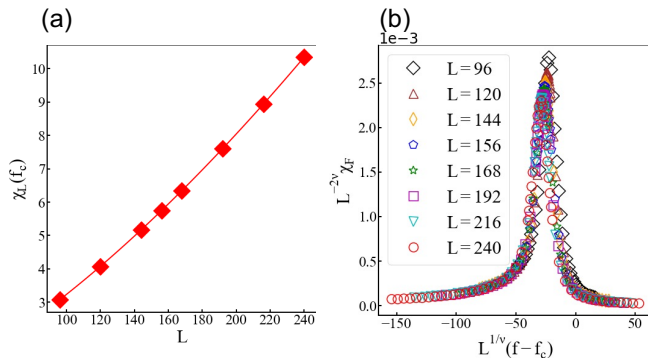


FIG. 3. (Color online) (a) The maximal of fidelity susceptibility per site $\chi_L(f_c^*) = \chi_F(f_c^*)/L$ as a function of system sizes L for $\alpha = 1.2$. We use polynomial fitting $\chi_L \sim L^\mu(a + bL^{-1})$ and extrapolate the critical adiabatic dimension $\mu = 2.53501$. (b) Data collapse of fidelity susceptibility χ_F for the Potts chain with long-range interaction; symbols denote the finite-size DMRG results for $\alpha = 1.2$ and $L = 96, 120, 144, 156, 168, 192, 216, 240$ sites, where $\nu = 0.78895$ and $f_c^* = 1.89878$ are used for data collapse plots.

by $L^{-2/\nu}\chi_F$ as a function of $L^\nu(f - f_c^*)$ in the vicinity of the quantum critical point f_c^* . The critical correlation length exponent $\nu (=0.78895)$ is then determined as the value at which all fidelity susceptibilities for different L collapse into a single one (Fig. 3(b)). The calculations of the critical adiabatic dimension μ and the correlation length exponent ν for other α are presented in Appendix C, and the results of all α are summarized in Table I. As can be seen from Fig. 4(a), either ν or μ as function of α shows a crossover at $\alpha = \alpha_c = 1.43$. When $\alpha < \alpha_c$, μ and ν are monotonic functions of α . In contrast, when $\alpha > \alpha_c$, they are more or less constant and approach the critical exponent values of the 2D three-state Potts model, $\nu = 5/6$ and $\mu = 12/5$, respectively, within 0.8% error due to finite size effect (black dash line in Fig. 4). Therefore, the critical behavior of the fidelity susceptibility undergoes a continuous crossover at $\alpha_c \approx 1.43$, from the long-range universality class region with varying correlation length exponent ($\alpha < \alpha_c$) to the short-range universality class region with constant exponents ($\alpha > \alpha_c$, three-state Potts region). This tendency is different from \mathbb{Z}_2 symmetric (Ising) quantum spin chain with long-range interaction [77, 78].

C. Discussion

The application of RG techniques to *classical* spin systems with long-range interactions provides a good understanding of phase transitions that occur within them. Perturbative two-loop RG calculations show that the three-state Potts chain with long-range power-law interactions has three parameter regimes, (1) small α ($\alpha < d/2$), (2) intermediate α ($d/2 < \alpha < \alpha_c$, and (3) large α ($\alpha > \alpha_c$) regions, similar to the classical three-state Potts model at low-energy and long-distance that can be described by ϕ^3 Landau-Ginzberg-Wilson effective action [42, 43]. Moreover, previous theoretical and

TABLE I. Critical exponents of the Potts chain with long-range interaction for different α . Critical exponents in the standard quantum Potts chain ($\alpha = \infty$) are also listed for comparison. The critical threshold of long-range interaction power $\alpha_c \sim 1.43$.

α	f_c^*	ν	μ
1.2	1.89878	0.78895	2.53501
1.3	1.78880	0.80400	2.48750
1.35	1.74389	0.81406	2.45681
1.4	1.69934	0.82796	2.41558
1.41	1.69227	0.82912	2.41220
1.42	1.68301	0.83255	2.40224
1.43	1.67415	0.83367	2.39903
1.44	1.66635	0.83658	2.39069
1.45	1.65914	0.83864	2.38481
1.5	1.61911	0.84018	2.38045
1.55	1.58752	0.83951	2.38223
1.6	1.55358	0.84251	2.37386
1.8	1.44159	0.84296	2.37258
2.0	1.35406	0.84007	2.38076
∞	1.00000	0.83333	2.40000

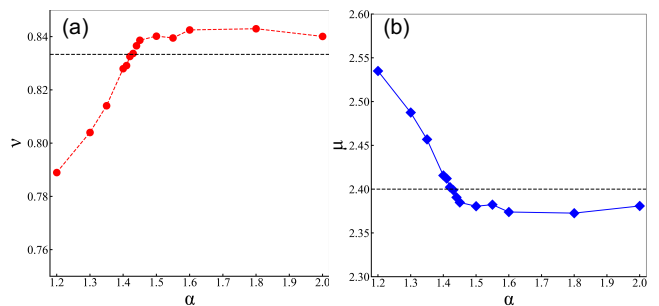


FIG. 4. (Color online) Critical exponent of the correlation length ν (black dash line refers to 2D three-state Potts correlation length exponent $\nu = 5/6$ as a comparison) (a) and critical adiabatic dimension μ (black dash line refers to 2D three-state Potts critical adiabatic dimension $\mu = 12/5$ as a comparison) (b) with respect to α for the Potts chain with long-range interaction; the symbols denote the finite-size DMRG results that are obtained by extrapolating from the fidelity susceptibility $\chi_F(f_c^*)$ at the peak position f_c^* of $L = 96, 120, 144, 156, 168, 192, 216, 240$ sites.

numerical results [39, 41, 77, 78] show that the critical behavior of $O(N)$ symmetric *quantum* model systems with long-range interactions is consistent with that of *classical* $O(N)$ ones with effective dimension $d_{\text{eff}} (= \frac{2d}{\alpha} + 1)$ for $d/2 < \alpha < \alpha_c$. However, for *quantum* systems with long-range interactions in the "non-classical" region ($d/2 < \alpha < \alpha_c$), the quantum-classical correspondence is very subtle and there is no analytical expression for the critical exponents. Particularly, it is unclear whether the critical behavior of the \mathbb{Z}_3 symmetric *quantum* spin systems with long-range interactions is also consistent with the two-loop RG results of the *classical* Potts model with long-range interactions.

For *quantum* three-state Potts model systems with long-range power-law interactions, using non-perturbative DMRG,

we found that there exists a critical value α_c in the long-range power-law interactions. When $\alpha < \alpha_c$, the RG flow ends in a stable long-range fixed point with varying critical exponents ν , and when $\alpha > \alpha_c$, it ends in a short-range fixed point. These results for *quantum* three-state Potts model systems with long-range power-law interactions are in qualitative agreement with previous two-loop RG results for *classical* ϕ^3 theory [42]. More importantly, for the first time, we numerically determine the critical threshold of the long-range interaction power $\alpha_c \approx 1.43$ in a non-perturbative manner, which is more accurate than previous perturbative two-loop RG results $\alpha_c \sim 1.73$.

IV. CONCLUSION

To summarize, we investigate the critical behavior of quantum Potts chain with long-range interactions through large-scale DMRG simulations. Using the fidelity susceptibility as a diagnostic, we obtain a ground-state phase diagram between PM and Potts order phases. As the long-range interaction power increases, the location of the quantum critical point shifts to weaker external fields. The finite-size scaling of the fidelity susceptibility χ_F and the nature of the QPTs of the quantum Potts chain with long-range interaction are also investigated. Our numerical results show that there is a critical threshold in the long-range interaction power, long-range fixed points are stable for $\alpha < \alpha_c$ and short-range fixed points are stable for $\alpha > \alpha_c$. These results are consistent with previous

two-loop RG calculations from classical ϕ^3 theory, but differ from the quantum Ising chains with long-range interaction. In addition, for the first time, we determined the critical long-range interaction power $\alpha_c \approx 1.43$ in a non-perturbative way, which is more precise than the previous perturbative two-loop RG results $\alpha_c \sim 1.73$. Interesting future questions include the fate of finite temperature effects in quantum Potts chains with long-range interaction, and the critical behavior of quantum four-state Potts models with long-range power interactions. Our work could shed new light on the interplay between long-range interactions (frustrated) and many-body physics.

ACKNOWLEDGMENTS

We thank Sheng Yang, and Nicolo Defenu for helpful discussions and communication. Numerical simulations were carried out with the ITensor package [79]. We also thank the computational resources provided by the TianHe-1A supercomputer, the High Performance Computing Platform of Peking University, China. This work is supported by National Natural Science Foundation of China under Grant No.11935002, and the National 973 project under Grant No. 2021YF1400501. C.D. was supported by the National Science Foundation of China under Grants No. 11975024, the Anhui Provincial Supporting Program for Excellent Young Talents in Colleges and Universities under Grant No. gxyqZD2019023.

-
- [1] John Cardy, *Scaling and renormalization in statistical physics*, Vol. 5 (Cambridge university press, 1996).
 - [2] Cenke Xu, "Unconventional quantum critical points," *International Journal of Modern Physics B* **26**, 1230007 (2012).
 - [3] Xue-Jia Yu, Peng-Lu Zhao, Shao-Kai Jian, and Zhiming Pan, "Emergent space-time supersymmetry at disordered quantum critical points," *Phys. Rev. B* **105**, 205140 (2022).
 - [4] Zheng-Xin Guo, Xue-Jia Yu, Xi-Dan Hu, and Zhi Li, "Emergent phase transitions in a cluster ising model with dissipation," *Phys. Rev. A* **105**, 053311 (2022).
 - [5] Subir Sachdev, *Quantum Phase Transitions*, 2nd ed. (Cambridge University Press, 2011).
 - [6] M. Saffman, T. G. Walker, and K. Mølmer, "Quantum information with rydberg atoms," *Rev. Mod. Phys.* **82**, 2313–2363 (2010).
 - [7] X.-L. Deng, D. Porras, and J. I. Cirac, "Effective spin quantum phases in systems of trapped ions," *Phys. Rev. A* **72**, 063407 (2005).
 - [8] T Lahaye, C Menotti, L Santos, M Lewenstein, and T Pfau, "The physics of dipolar bosonic quantum gases," *Reports on Progress in Physics* **72**, 126401 (2009).
 - [9] M. Saffman, T. G. Walker, and K. Mølmer, "Quantum information with rydberg atoms," *Rev. Mod. Phys.* **82**, 2313–2363 (2010).
 - [10] Helmut Ritsch, Peter Domokos, Ferdinand Brennecke, and Tilman Esslinger, "Cold atoms in cavity-generated dynamical optical potentials," *Rev. Mod. Phys.* **85**, 553–601 (2013).
 - [11] Lincoln D Carr, David DeMille, Roman V Krems, and Jun Ye, "Cold and ultracold molecules: science, technology and applications," *New Journal of Physics* **11**, 055049 (2009).
 - [12] Rainer Blatt and Christian F Roos, "Quantum simulations with trapped ions," *Nature Physics* **8**, 277–284 (2012).
 - [13] Joseph W Britton, Brian C Sawyer, Adam C Keith, C-C Joseph Wang, James K Freericks, Hermann Uys, Michael J Biercuk, and John J Bollinger, "Engineered two-dimensional ising interactions in a trapped-ion quantum simulator with hundreds of spins," *Nature* **484**, 489–492 (2012).
 - [14] R Islam, Crystal Senko, Wes C Campbell, S Korenblit, J Smith, A Lee, EE Edwards, C-CJ Wang, JK Freericks, and C Monroe, "Emergence and frustration of magnetism with variable-range interactions in a quantum simulator," *science* **340**, 583–587 (2013).
 - [15] Philip Richerme, Zhe-Xuan Gong, Aaron Lee, Crystal Senko, Jacob Smith, Michael Foss-Feig, Spyridon Michalakis, Alexey V Gorshkov, and Christopher Monroe, "Non-local propagation of correlations in quantum systems with long-range interactions," *Nature* **511**, 198–201 (2014).
 - [16] Petar Jurcevic, Ben P Lanyon, Philipp Hauke, Cornelius Hempel, Peter Zoller, Rainer Blatt, and Christian F Roos, "Quasiparticle engineering and entanglement propagation in a quantum many-body system," *Nature* **511**, 202–205 (2014).
 - [17] Menghan Song, Jiarui Zhao, Chengkang Zhou, and Zi Yang Meng, "Dynamical properties of quantum many-body systems with long range interactions," (2023).
 - [18] Ruben Verresen, Mikhail D. Lukin, and Ashvin Vishwanath, "Prediction of toric code topological order from rydberg blockade," *Phys. Rev. X* **11**, 031005 (2021).

- [19] Rhine Samajdar, Darshan G. Joshi, Yanting Teng, and Subir Sachdev, “Emergent Z_2 gauge theories and topological excitations in rydberg atom arrays,” (2022).
- [20] Giulia Semeghini, Harry Levine, Alexander Keesling, Sepehr Ebadi, Tout T Wang, Dolev Bluvstein, Ruben Verresen, Hannes Pichler, Marcin Kalinowski, Rhine Samajdar, *et al.*, “Probing topological spin liquids on a programmable quantum simulator,” *Science* **374**, 1242–1247 (2021).
- [21] Rhine Samajdar, Wen Wei Ho, Hannes Pichler, Mikhail D Lukin, and Subir Sachdev, “Quantum phases of rydberg atoms on a kagome lattice,” *Proceedings of the National Academy of Sciences* **118** (2021).
- [22] Kevin Slagle, Yue Liu, David Aasen, Hannes Pichler, Roger S. K. Mong, Xie Chen, Manuel Endres, and Jason Alicea, “Quantum spin liquids bootstrapped from ising criticality in rydberg arrays,” (2022).
- [23] Yanting Cheng, Chengshu Li, and Hui Zhai, “Variational approach to quantum spin liquid in a rydberg atom simulator,” (2021).
- [24] Rhine Samajdar, Wen Wei Ho, Hannes Pichler, Mikhail D. Lukin, and Subir Sachdev, “Complex density wave orders and quantum phase transitions in a model of square-lattice rydberg atom arrays,” *Phys. Rev. Lett.* **124**, 103601 (2020).
- [25] Rhine Samajdar, Soonwon Choi, Hannes Pichler, Mikhail D. Lukin, and Subir Sachdev, “Numerical study of the chiral F_3 quantum phase transition in one spatial dimension,” *Phys. Rev. A* **98**, 023614 (2018).
- [26] Seth Whitsitt, Rhine Samajdar, and Subir Sachdev, “Quantum field theory for the chiral clock transition in one spatial dimension,” *Phys. Rev. B* **98**, 205118 (2018).
- [27] Marcin Kalinowski, Rhine Samajdar, Roger G. Melko, Mikhail D. Lukin, Subir Sachdev, and Soonwon Choi, “Bulk and boundary quantum phase transitions in a square rydberg atom array,” (2021).
- [28] Matthew J. O’Rourke and Garnet Kin-Lic Chan, “Entanglement in the quantum phases of an unfrustrated rydberg atom array,” (2022).
- [29] Ejaaz Merali, Isaac J. S. De Vlucht, and Roger G. Melko, “Stochastic series expansion quantum monte carlo for rydberg arrays,” (2021).
- [30] Kevin Slagle, David Aasen, Hannes Pichler, Roger S. K. Mong, Paul Fendley, Xie Chen, Manuel Endres, and Jason Alicea, “Microscopic characterization of ising conformal field theory in rydberg chains,” *Phys. Rev. B* **104**, 235109 (2021).
- [31] Jason Alicea and Paul Fendley, “Topological phases with parafermions: theory and blueprints,” *Annual Review of Condensed Matter Physics* **7**, 119–139 (2016).
- [32] Paul Fendley, “Parafermionic edge zero modes in Z_n -invariant spin chains,” *Journal of Statistical Mechanics: Theory and Experiment* **2012**, P11020 (2012).
- [33] Edward O’Brien, Eric Vernier, and Paul Fendley, ““not-a”, representation symmetry-protected topological, and potts phases in an S_3 -invariant chain,” *Phys. Rev. B* **101**, 235108 (2020).
- [34] Ye Zhuang, Hitesh J. Changlani, Norm M. Tubman, and Taylor L. Hughes, “Phase diagram of the Z_3 parafermionic chain with chiral interactions,” *Phys. Rev. B* **92**, 035154 (2015).
- [35] Edward O’Brien and Paul Fendley, “Self-dual S_3 -invariant quantum chains,” *SciPost Phys.* **9**, 88 (2020).
- [36] Xue-Jia Yu, Rui-Zhen Huang, Hong-Hao Song, Limei Xu, Chengxiang Ding, and Long Zhang, “Conformal boundary conditions of symmetry-enriched quantum critical spin chains,” *Phys. Rev. Lett.* **129**, 210601 (2022).
- [37] Abolhassan Vaezi, “Superconducting analogue of the parafermion fractional quantum hall states,” *Phys. Rev. X* **4**, 031009 (2014).
- [38] Wei Li, Shuo Yang, Hong-Hao Tu, and Meng Cheng, “Criticality in translation-invariant parafermion chains,” *Phys. Rev. B* **91**, 115133 (2015).
- [39] Michael E. Fisher, Shang-keng Ma, and B. G. Nickel, “Critical exponents for long-range interactions,” *Phys. Rev. Lett.* **29**, 917–920 (1972).
- [40] Michael Knap, Adrian Kantian, Thierry Giamarchi, Immanuel Bloch, Mikhail D. Lukin, and Eugene Demler, “Probing real-space and time-resolved correlation functions with many-body Ramsey interferometry,” *Phys. Rev. Lett.* **111**, 147205 (2013).
- [41] Nicolò Defenu, Andrea Trombettoni, and Stefano Ruffo, “Criticality and phase diagram of quantum long-range $o(n)$ models,” *Phys. Rev. B* **96**, 104432 (2017).
- [42] W. K. Theumann and M. A. Gusmo, “Critical exponents for φ^3 -field models with long-range interactions,” *Phys. Rev. B* **31**, 379–388 (1985).
- [43] Nicolò Defenu, Tobias Donner, Tommaso Macrì, Guido Pagano, Stefano Ruffo, and Andrea Trombettoni, “Long-range interacting quantum systems,” (2021).
- [44] Nicolò Defenu, Andrea Trombettoni, and Alessandro Codello, “Fixed-point structure and effective fractional dimensionality for $o(n)$ models with long-range interactions,” *Phys. Rev. E* **92**, 052113 (2015).
- [45] Edouard Brezin, Giorgio Parisi, and Federico Ricci-Tersenghi, “The crossover region between long-range and short-range interactions for the critical exponents,” *Journal of Statistical Physics* **157**, 855–868 (2014).
- [46] Maria Chiara Angelini, Giorgio Parisi, and Federico Ricci-Tersenghi, “Relations between short-range and long-range ising models,” *Phys. Rev. E* **89**, 062120 (2014).
- [47] Connor Behan, Leonardo Rastelli, Slava Rychkov, and Bernardo Zan, “Long-range critical exponents near the short-range crossover,” *Phys. Rev. Lett.* **118**, 241601 (2017).
- [48] Connor Behan, Leonardo Rastelli, Slava Rychkov, and Bernardo Zan, “A scaling theory for the long-range to short-range crossover and an infrared duality,” *Journal of Physics A: Mathematical and Theoretical* **50**, 354002 (2017).
- [49] Philippe Francesco, Pierre Mathieu, and David Sénéchal, *Conformal field theory* (Springer Science & Business Media, 2012).
- [50] Paul Ginsparg, “Applied conformal field theory,” (1991), 10.48550/ARXIV.HEP-TH/9108028.
- [51] Wing Chi Yu, Shi-Jian Gu, and Hai-Qing Lin, “Fidelity susceptibilities in the one-dimensional extended Hubbard model,” (2014).
- [52] A. Fabricio Albuquerque, Fabien Alet, Clément Sire, and Sylvain Capponi, “Quantum critical scaling of fidelity susceptibility,” *Phys. Rev. B* **81**, 064418 (2010).
- [53] David Schwandt, Fabien Alet, and Sylvain Capponi, “Quantum monte carlo simulations of fidelity at magnetic quantum phase transitions,” *Phys. Rev. Lett.* **103**, 170501 (2009).
- [54] Wing-Chi Yu, Ho-Man Kwok, Junpeng Cao, and Shi-Jian Gu, “Fidelity susceptibility in the two-dimensional transverse-field ising and xzx models,” *Phys. Rev. E* **80**, 021108 (2009).
- [55] G. Sun, A. K. Kolezhuk, and T. Vekua, “Fidelity at berezinskii-kosterlitz-thouless quantum phase transitions,” *Phys. Rev. B* **91**, 014418 (2015).
- [56] E. J. König, A. Levchenko, and N. Sedlmayr, “Universal fidelity near quantum and topological phase transitions in finite one-dimensional systems,” *Phys. Rev. B* **93**, 235160 (2016).
- [57] Bo-Bo Wei, “Fidelity susceptibility in one-dimensional disordered lattice models,” *Phys. Rev. A* **99**, 042117 (2019).
- [58] Ting Lv, Tian-Cheng Yi, Liangsheng Li, Gaoyong Sun, and Wen-Long You, “Quantum criticality and universality in the

- p -wave-paired aubry-andré-harper model,” *Phys. Rev. A* **105**, 013315 (2022).
- [59] Xue-Jia Yu, Sheng Yang, Jing-Bo Xu, and Limei Xu, “Fidelity susceptibility as a diagnostic of the commensurate-incommensurate transition: A revisit of the programmable rydberg chain,” *Phys. Rev. B* **106**, 165124 (2022).
- [60] Gaoyong Sun, Bo-Bo Wei, and Su-Peng Kou, “Fidelity as a probe for a deconfined quantum critical point,” *Phys. Rev. B* **100**, 064427 (2019).
- [61] Yi-Ting Tu, Iksu Jang, Po-Yao Chang, and Yu-Chin Tzeng, “General properties of fidelity in non-hermitian quantum systems with pt symmetry,” (2022).
- [62] Gaoyong Sun, Jia-Chen Tang, and Su-Peng Kou, “Biorthogonal quantum criticality in non-hermitian many-body systems,” *Frontiers of Physics* **17**, 1–9 (2022).
- [63] Shi-Jian Gu and Wing Chi Yu, “Spectral function and fidelity susceptibility in quantum critical phenomena,” *EPL (Europhysics Letters)* **108**, 20002 (2014).
- [64] Shi-Jian Gu, “Fidelity approach to quantum phase transitions,” *International Journal of Modern Physics B* **24**, 4371–4458 (2010).
- [65] Shi-Jian Gu, “Fidelity susceptibility and quantum adiabatic condition in thermodynamic limits,” *Phys. Rev. E* **79**, 061125 (2009).
- [66] Shi-Jian Gu and Hai-Qing Lin, “Scaling dimension of fidelity susceptibility in quantum phase transitions,” *EPL (Europhysics Letters)* **87**, 10003 (2009).
- [67] Wen-Long You and Li He, “Generalized fidelity susceptibility at phase transitions,” *Journal of Physics: Condensed Matter* **27**, 205601 (2015).
- [68] Steven R. White, “Density matrix formulation for quantum renormalization groups,” *Phys. Rev. Lett.* **69**, 2863–2866 (1992).
- [69] U. Schollwöck, “The density-matrix renormalization group,” *Rev. Mod. Phys.* **77**, 259–315 (2005).
- [70] Ulrich Schollwöck, “The density-matrix renormalization group in the age of matrix product states,” *Annals of Physics* **326**, 96–192 (2011), january 2011 Special Issue.
- [71] F. Verstraete, D. Porras, and J. I. Cirac, “Density matrix renormalization group and periodic boundary conditions: A quantum information perspective,” *Phys. Rev. Lett.* **93**, 227205 (2004).
- [72] J. Sólyom and P. Pfeuty, “Renormalization-group study of the hamiltonian version of the potts model,” *Phys. Rev. B* **24**, 218–229 (1981).
- [73] Rui-Zhen Huang and Shuai Yin, “Nonequilibrium critical dynamics in the quantum chiral clock model,” *Phys. Rev. B* **99**, 184104 (2019).
- [74] H.J. Lipkin, N. Meshkov, and A.J. Glick, “Validity of many-body approximation methods for a solvable model: (i). exact solutions and perturbation theory,” *Nuclear Physics* **62**, 188–198 (1965).
- [75] Bogdan Damski, “Fidelity approach to quantum phase transitions in quantum ising model,” in *Quantum Criticality in Condensed Matter: Phenomena, Materials and Ideas in Theory and Experiment* (World Scientific, 2016) pp. 159–182.
- [76] Anders W Sandvik, “Computational studies of quantum spin systems,” in *AIP Conference Proceedings*, Vol. 1297 (American Institute of Physics, 2010) pp. 135–338.
- [77] Gaoyong Sun, “Fidelity susceptibility study of quantum long-range antiferromagnetic ising chain,” *Phys. Rev. A* **96**, 043621 (2017).
- [78] Zhangqi Zhu, Gaoyong Sun, Wen-Long You, and Da-Ning Shi, “Fidelity and criticality of a quantum ising chain with long-range interactions,” *Phys. Rev. A* **98**, 023607 (2018).

- [79] Matthew Fishman, Steven R. White, and E. Miles Stoudenmire, “The itensor software library for tensor network calculations,” (2020).

Appendix A: FIDELITY SUSCEPTIBILITY FOR OTHER INTERACTION POWERS

In this section, we provide additional data to show fidelity susceptibility for other interaction powers.

As the same in the main text, on the one hand, fidelity susceptibility per site χ_L of the Potts chain with long-range interaction for $\alpha = 1.3$ (a), $\alpha = 1.35$ (b), $\alpha = 1.4$ (c), $\alpha = 1.5$ (d), $\alpha = 1.55$ (e), $\alpha = 1.6$ (f), $\alpha = 1.8$ (g), $\alpha = 2.0$ (h), and $L = 96, 120, 144, 156, 168, 192, 216, 240$ sites as a function of external transverse field f , are shown in the Fig. 5. On the other hand, in order to determine critical α_c , we also show fidelity susceptibility per site for $\alpha = 1.41$ (a), $\alpha = 1.42$ (b), $\alpha = 1.43$ (c), $\alpha = 1.44$ (d), $\alpha = 1.45$ (e) in the Fig. 6. We find that quantum critical points are shifted to lower values of f as long-range interaction power increases.

Appendix B: DATA COLLAPES FOR OTHER INTERACTION POWERS

In this section, we provide additional data to show that the varying tendency of long-range correlation length exponents in the "non-classical" region is consistent with theoretical analysis.

As the same in the main text, on the one hand, data collapse of fidelity susceptibility chi_F for the Potts chain with long-range interaction, $\alpha = 1.3$ (a), $\alpha = 1.35$ (b), $\alpha = 1.4$ (c), $\alpha = 1.5$ (d), $\alpha = 1.55$ (e), $\alpha = 1.6$ (f), $\alpha = 1.8$ (g), $\alpha = 2.0$ (h), and $L = 96, 120, 144, 156, 168, 192, 215, 240$ sites, are shown in Fig. 7. On the other hand, in order to determine critical α_c , we also show data collapse for $\alpha = 1.41$ (a), $\alpha = 1.42$ (b), $\alpha = 1.43$ (c), $\alpha = 1.44$ (d), $\alpha = 1.45$ (e) in the Fig. 8. The correlation length exponents are summarized in Table. I. We clearly see that the varying tendency of correlation length exponents in the "non-classical" region is consistent with the theoretical analysis.

Appendix C: QUANTUM ADIABATIC DIMENSION FITTING FOR OTHER INTERACTION POWERS

In this section, we provide additional data to extrapolate critical adiabatic dimensions for other long-range interaction powers.

As the same in the main text, on the one hand, the maximal of fidelity susceptibility per site $\chi_L(f_c^*) = \chi_F(f_c^*)/L$ as a function of system sizes L for $\alpha = 1.3$ (a), $\alpha = 1.35$ (b), $\alpha = 1.4$ (c), $\alpha = 1.5$ (d), $\alpha = 1.55$ (e), $\alpha = 1.6$ (f), $\alpha = 1.8$ (g), $\alpha = 2.0$ (h), and $L = 96, 120, 144, 156, 168, 192, 216, 240$ sites, are shown in Fig. 9. On the other hand, in order to determine critical α_c , we also show the maximal of fidelity susceptibility per site for $\alpha = 1.41$ (a), $\alpha = 1.42$ (b), $\alpha =$

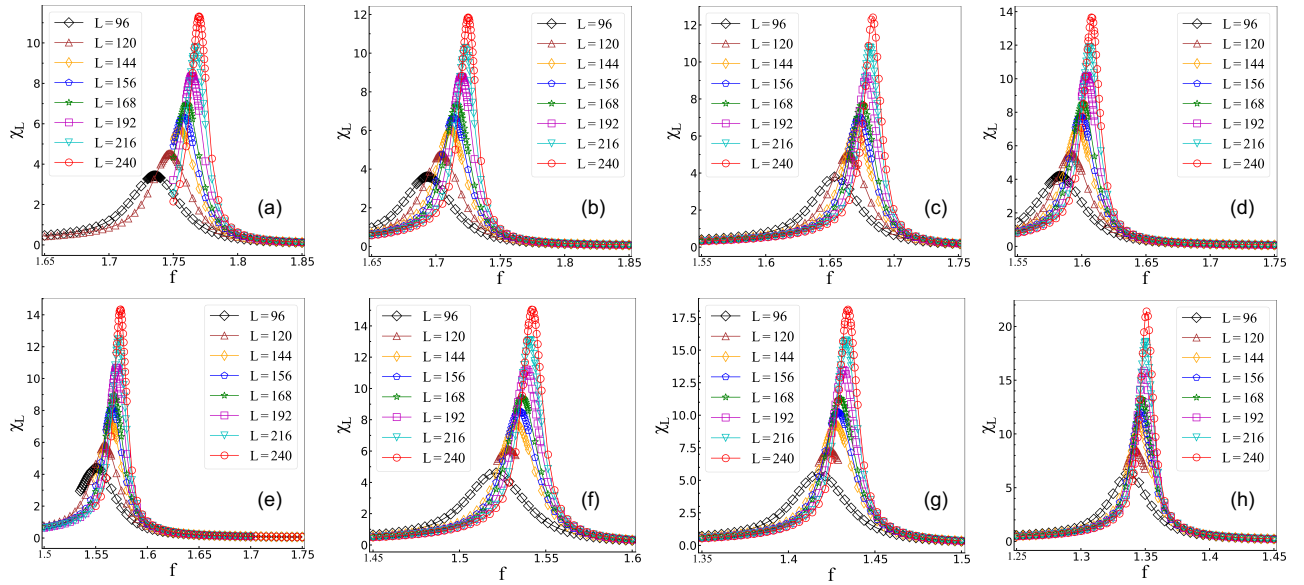


FIG. 5. (Color online) Fidelity susceptibility per site χ_L of the Potts chain with long-range interaction for (a) $\alpha = 1.3$, (b) $\alpha = 1.35$, (c) $\alpha = 1.4$, (d) $\alpha = 1.5$, (e) $\alpha = 1.55$, (f) $\alpha = 1.6$, (g) $\alpha = 1.8$, (h) $\alpha = 2.0$, and $L = 96, 120, 144, 156, 168, 192, 216, 240$ sites as a function of external transverse field f ; symbols denote finite-size DMRG results.

1.43 (c), $\alpha = 1.44$ (d), $\alpha = 1.45$ (e) in the Fig. 10. The critical adiabatic dimensions are summarized in the Table. I. We clearly see that the varying tendency of critical adiabatic dimension in the "non-classical" region is consistent with the theoretical analysis.

Appendix D: QUANTUM CRITICAL POINT FITTING FOR OTHER INTERACTION POWERS

In this section, we provide additional data to extrapolate accuracy critical points for other long-range interaction powers.

As the same in the main text, on the one hand, the finite-size scaling of pseudo-critical point $f_c(L)$ as a function of inverse system sizes $1/L$ for $\alpha = 1.3$ (a), $\alpha = 1.35$ (b), $\alpha = 1.4$ (c), $\alpha = 1.5$ (d), $\alpha = 1.55$ (e), $\alpha = 1.6$ (f), $\alpha = 1.8$ (g), $\alpha = 2.0$ (h), and $L = 96, 120, 144, 156, 168, 192, 216, 240$ sites, are shown in Fig. 11. On the other hand, in order to determine critical α_c , we also show the finite-size scaling of pseudo-critical point as a function of inverse system sizes for $\alpha = 1.41$ (a), $\alpha = 1.42$ (b), $\alpha = 1.43$ (c), $\alpha = 1.44$ (d), $\alpha = 1.45$ (e) in the Fig. 12. The extrapolated critical points are summarized in Table. I. We clearly see that the critical point f_c^* shifts to weaker values with increasing α .

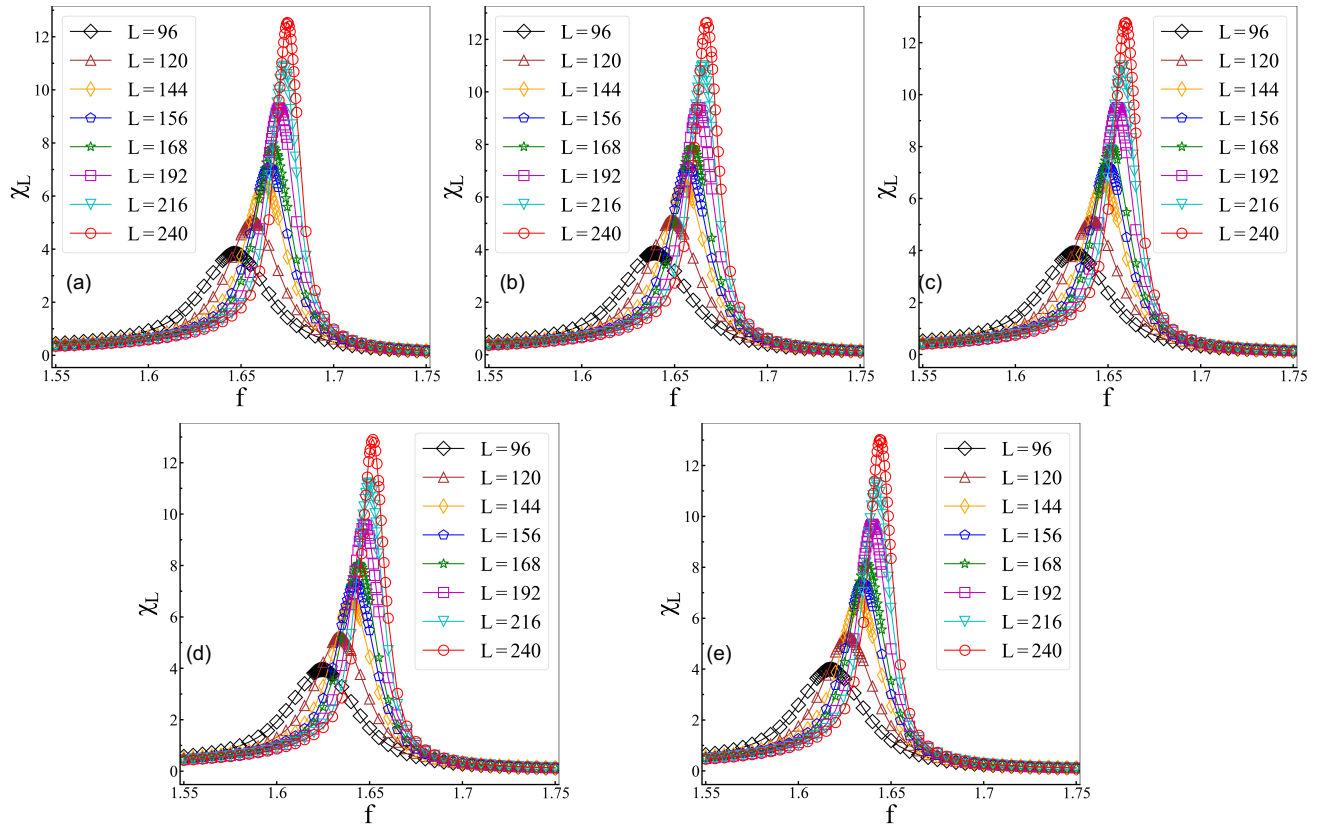


FIG. 6. (Color online) Fidelity susceptibility per site χ_L of the Potts chain with long-range interaction for (a) $\alpha = 1.41$, (b) $\alpha = 1.42$, (c) $\alpha = 1.43$, (d) $\alpha = 1.44$, (e) $\alpha = 1.45$, and $L = 96, 120, 144, 156, 168, 192, 216, 240$ sites as a function of external transverse field f ; symbols denote finite-size DMRG results.

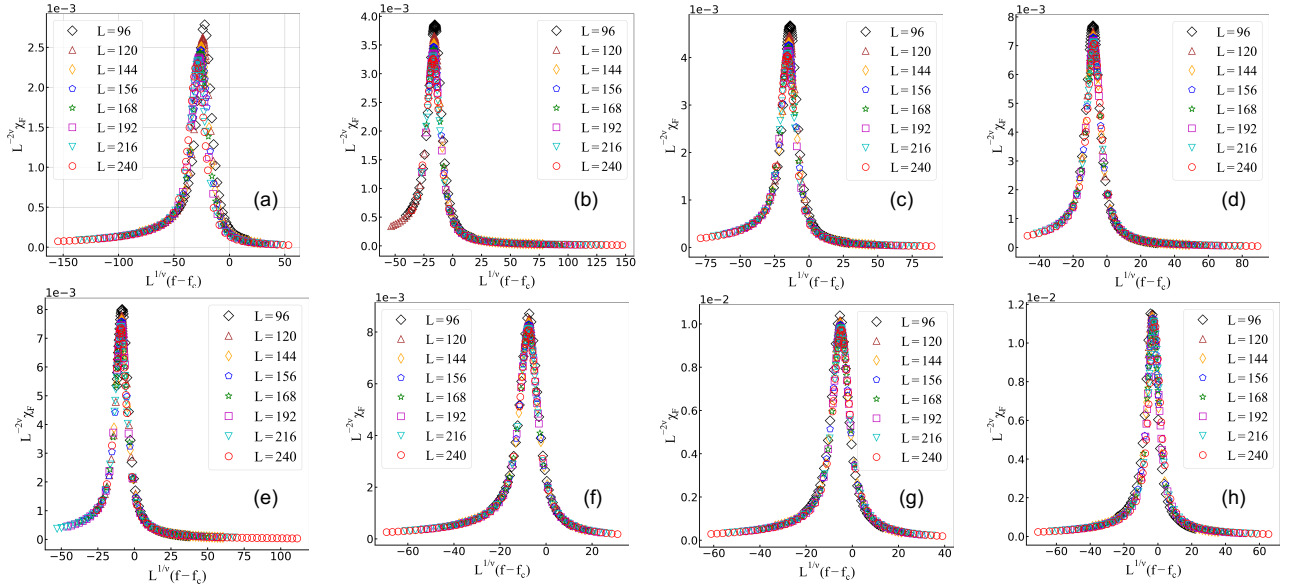


FIG. 7. (Color online) Data collapse of fidelity susceptibility χ_f for the Potts chain with long-range interaction; symbols denote the finite-size DMRG results for (a) $\alpha = 1.3$, (b) $\alpha = 1.35$, (c) $\alpha = 1.4$, (d) $\alpha = 1.5$, (e) $\alpha = 1.55$, (f) $\alpha = 1.6$, (g) $\alpha = 1.8$, (h) $\alpha = 2.0$, where the varying tendency of correlation length exponents in the "non-classical" region is consistent with the theoretical analysis.

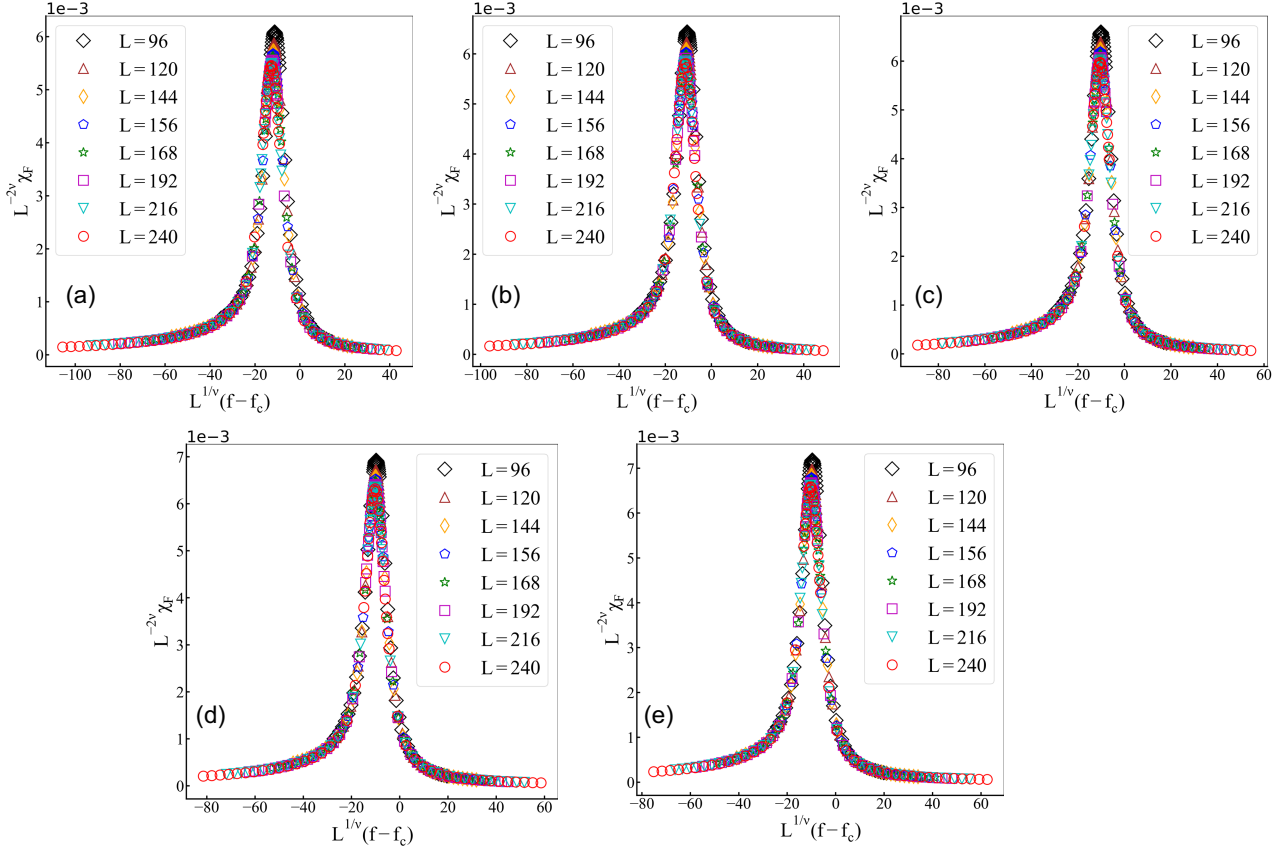


FIG. 8. (Color online) Data collapse of fidelity susceptibility χ_F for the Potts chain with long-range interaction; symbols denote the finite-size DMRG results for (a) $\alpha = 1.41$, (b) $\alpha = 1.42$, (c) $\alpha = 1.43$, (d) $\alpha = 1.44$, (e) $\alpha = 1.45$, where the varying tendency of correlation length exponents in the "non-classical" region is consistent with the theoretical analysis.

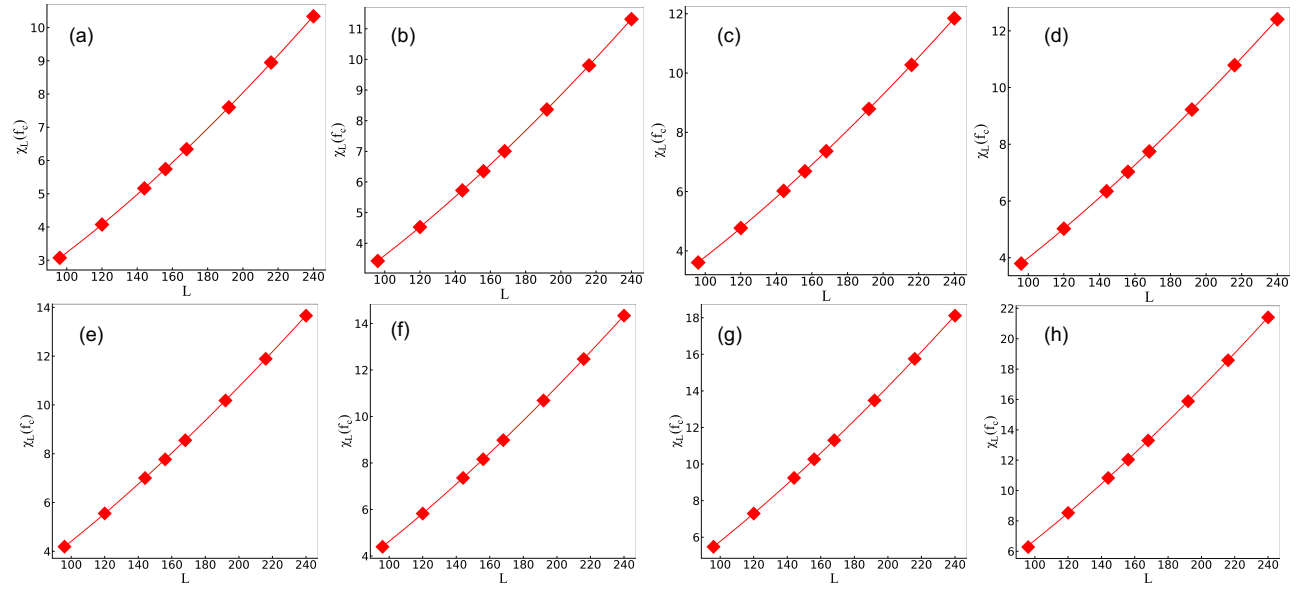


FIG. 9. (Color online) The maximal of fidelity susceptibility per site $\chi_L(f_c^*) = \chi_F(f_c^*)/L$ as a function of system sizes L for (a) $\alpha = 1.3$, (b) $\alpha = 1.35$, (c) $\alpha = 1.4$, (d) $\alpha = 1.5$, (e) $\alpha = 1.55$, (f) $\alpha = 1.6$, (g) $\alpha = 1.8$, (h) $\alpha = 2.0$. We use polynomial fitting formula: $\chi_L(f_c^*) = L^\mu(a + bL^{-1})$

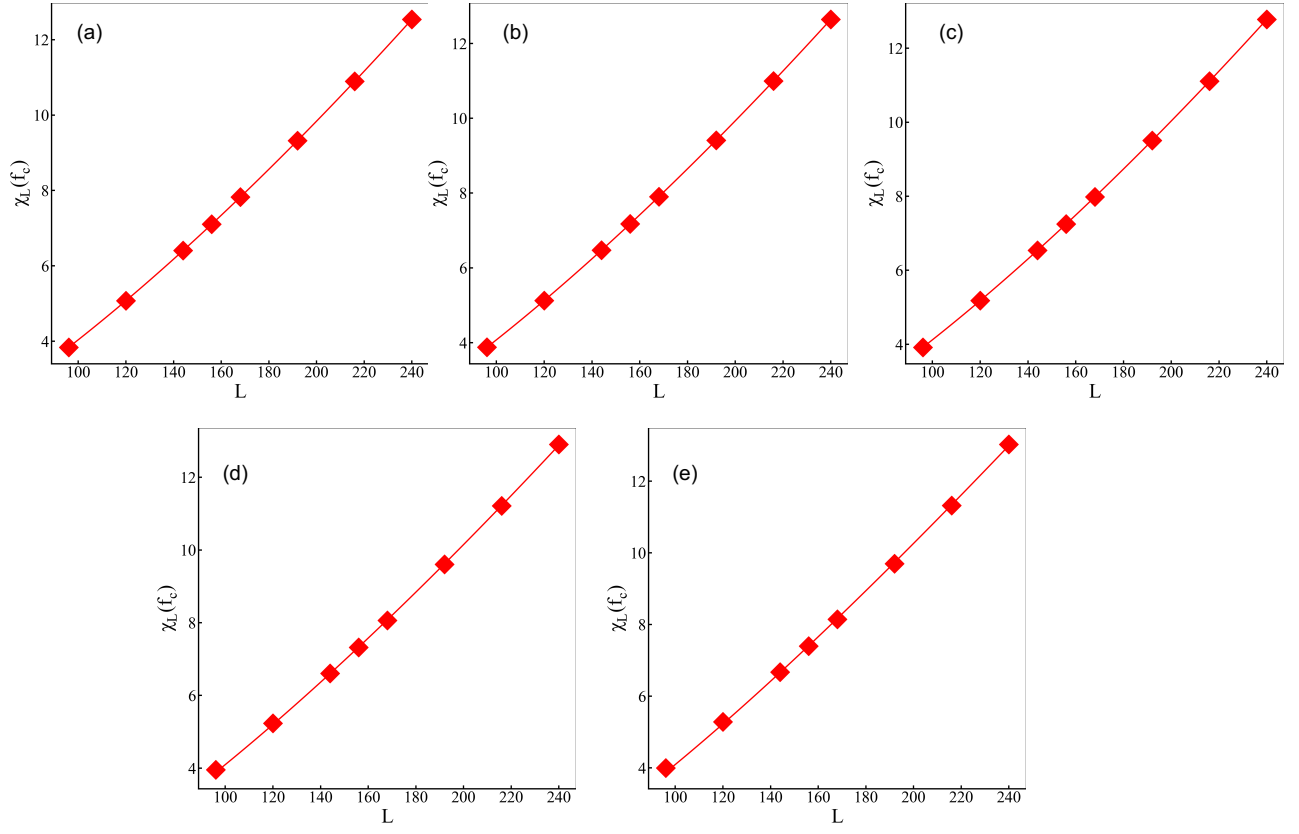


FIG. 10. (Color online) The maximal of fidelity susceptibility per site as a function of system sizes L for (a) $\alpha = 1.41$, (b) $\alpha = 1.42$, (c) $\alpha = 1.43$, (d) $\alpha = 1.43$, (e) $\alpha = 1.45$. We use polynomial fitting formula: $\chi_L(f_c^*) = L^\mu(a + bL^{-1})$

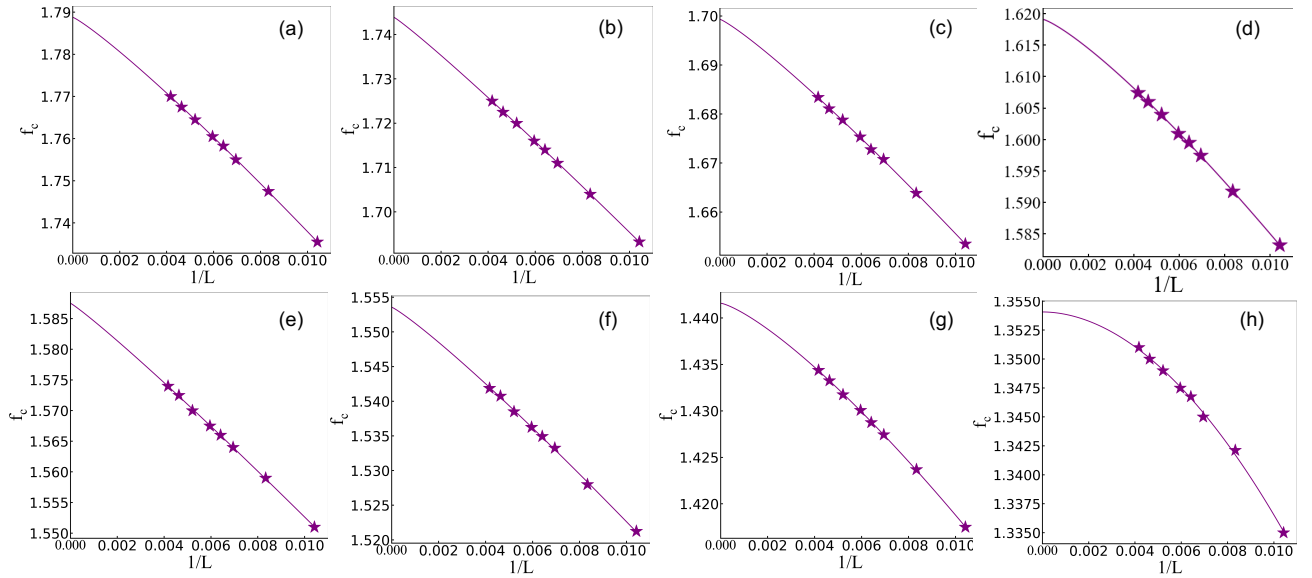


FIG. 11. (Color online) The finite size scaling of pseudo-critical point $f_c(L)$ as a function of inverse system sizes $1/L$ for (a) $\alpha = 1.3$, (b) $\alpha = 1.35$, (c) $\alpha = 1.4$, (d) $\alpha = 1.5$, (e) $\alpha = 1.55$, (f) $\alpha = 1.6$, (g) $\alpha = 1.8$, (h) $\alpha = 2.0$. We use polynomial fitting formula: $\chi_L(f_c^*) = L^\mu(a + bL^{-1})$

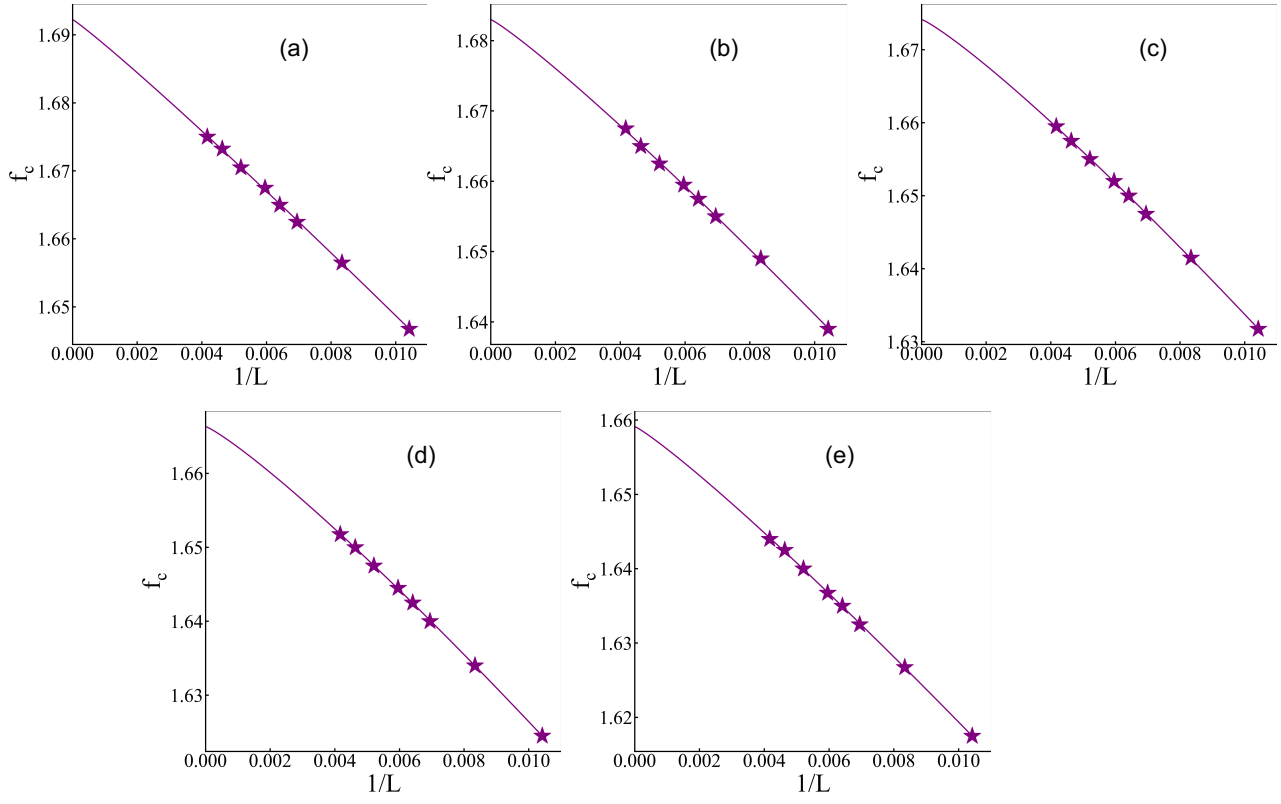


FIG. 12. (Color online) The finite size scaling of pseudo-critical point $f_c(L)$ as a function of inverse system sizes $1/L$ for (a) $\alpha = 1.41$, (b) $\alpha = 1.42$, (c) $\alpha = 1.43$, (d) $\alpha = 1.44$, (e) $\alpha = 1.45$. We use polynomial fitting formula: $\chi_L(f_c^*) = L^\mu(a + bL^{-1})$